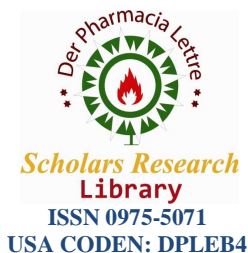




Scholars Research Library

Der Pharmacia Lettre, 2016, 8 (17):215-222
(<http://scholarsresearchlibrary.com/archive.html>)



A Quantum-Chemical study of the Relationships between Electronic Structure and Trypanocidal Activity against *Trypanosoma Brucei Brucei* of a series of Thiosemicarbazone derivatives

Gaston Kpotin*¹, Sylvain Y. G. Atohoun¹, Urbain A. Kuevi¹, Alice Kpota-Houngue¹, Jean-Baptiste Mensah¹ and Juan S. Gómez-Jeria²

¹Laboratory of Theoretical Chemistry and Molecular Spectroscopy, Faculty of Sciences and Technic, University of Abomey-Calavi, 03 BP 3409 Cotonou-Benin

²Quantum Pharmacology Unit, Department of Chemistry, Faculty of Sciences, University of Chile. Las Palmeras 3425, Santiago 7800003, Chile

ABSTRACT

A study of the relationships between electronic structure and trypanocidal activities of a series of thiosemicarbazone derivatives on *Trypanosoma brucei brucei* was carried out. With the log (IC_{50}) of the biological activity and the variation of the values of set of twenty local atomic reactivity indices belonging to common skeleton, we obtain one statistically significant equation ($R= 0.98$, $R^2= 0.96$, $adj-R^2= 0.93$, $F(7,12)=39.20$ ($p<0.00000$), $SD= 0.12$). Based on the analysis of the results, a partial two-dimensional trypanocidal pharmacophore was built.

Keywords: *Trypanosoma brucei brucei*, thiosemicarbazone derivatives, QSAR, pharmacophore, DFT, QSAR.

INTRODUCTION

African trypanosomes are flagellated protozoa living extracellularly in blood and tissues of the mammalian hosts and are transmitted by the bite of tsetse flies (*Glossina* spp)[1, 2]. It is a protozoan parasite that affects humans as well as animals [3] and is responsible for sleeping sickness. While *Trypanosoma brucei brucei* decimates livestock, *Trypanosoma brucei gambiense* and *Trypanosoma brucei rhodesiense* species are responsible for human African trypanosomiasis. In 2009, after continued control efforts, the number of cases reported dropped below 10,000 (9878) for the first time in 50 years. This decline in number of cases has continued with 6314 new cases reported in 2012. However, the estimated number of actual cases is about 20,000 and the estimated population at risk is 65 million people[4]. These diseases represent a major public health problem in region of the world least able to deal with the associated economic burden. With no immediate prospect of vaccines, and no satisfactory drug treatments, the requirement for new therapies is a priority. However, drug discovery is high risk and expensive, and the development of agents designed specifically to target trypanosomal diseases is not perceived to be commercially attractive [5]. In fact, among these drugs, few of them are available for chemotherapy and most are outdated and difficult to administer [2, 6]. Drugs used for the treatment of human African trypanosomiasis we have Suramin, Pentamidine, Melarsoprol and Eflornithine. Each of these drugs presents one or some problems such as ineffective against early stage, ineffective against late stage, toxic, resistance observed in field [5]. A recent study shows that thiosemicarbazones have antibacterial [7, 8], antimicrobial [9], antiviral [10], antitumor [11-13] and antifungal [14] activities. Furthermore, some works show that they possess trypanocidal activities [1-3, 15,

16]. Thiosemicarbazones are DNA replication and protease inhibitors [3], particularly cysteine protease inhibitors [1, 14, 17, 18]. This inhibitory activity justifies the study of the trypanocidal activity because cysteine protease inhibitors have been shown to kill African trypanosoma *in vitro* and in animal models of disease [19, 20]. In this paper we present the results of a quantum-chemical study of the relationships between electronic structure and trypanocidal activities against *Trypanosoma brucei brucei* of a series of thiosemicarbazone derivatives.

METHODS AND CALCULATIONS

The model.

As the methodology employed here to find relationships between electronic structure and inhibition constants has been extensively discussed and applied in several papers, we present here a short standard summary [21-28]. The inhibition constant, IC_{50} can be expressed as a linear relationship of the form:

$$\log(IC_{50}) = a + \sum_j [e_j Q_j + f_j S_j^E + s_j S_j^N] + \sum_j \sum_m [h_j(m) F_j(m) + x_j(m) S_j^E(m)] + \sum_j \sum_{m'} [r_j(m') F_j(m') + t_j(m') S_j^N(m')] + \sum_j [g_j \mu_j + k_j \eta_j + o_j \omega_j + z_j \zeta_j + w_j Q_j^{\max}] + \sum_{k=1}^U O_k \quad (1)$$

where Q_j is the net charge of atom j , S_j^E and S_j^N are, respectively, the total atomic electrophilic and nucleophilic superdelocalizabilities of Fukui *et al.*, $F_{j,m}$ ($F_{j,m'}$) is Fukui index of the occupied (vacant) MO m (m') located on atom j [29]. $S_j^E(m)$ is the atomic electrophilic superdelocalizability of MO m on atom j , etc. The total atomic electrophilic superdelocalizability of atom j corresponds to the sum over occupied MOs of the $S_j^E(m)$'s and the total atomic nucleophilic superdelocalizability of atom j is the sum over vacant MOs of $S_j^N(m')$'s [29]. μ_j is the local atomic electronic chemical potential of atom j , η_j is the local atomic hardness of atom j , ω_j is the local atomic electrophilicity of atom j , ζ_j is the local atomic softness of atom j , and Q_j^{\max} is the maximum amount of electronic charge that atom j may accept from another site [26, 27]. O_k 's are the orientational parameters of the substituents [30-32]. Throughout this paper $HOMO_j^*$ refers to the highest occupied molecular orbital localized on atom j and $LUMO_j^*$ to the lowest empty MO localized on atom j . They are called the local atomic frontier MOs. The application of this method (Eq. 1) has given exceptional results for a great diversity of drug-receptor systems (see [33-44] and references therein).

Selection of the experimental data.

Molecules were selected from a set reported in Ref. [3]. The molecules are shown in Fig.1 and Table 1. The experimental data employed in this study are the trypanocidal activity on *Trypanosoma brucei brucei*, IC_{50} . The test is performed on the bloodstream form of the strain 427 of *Trypanosoma brucei brucei* by the Lilit Alamar Blue method [3].

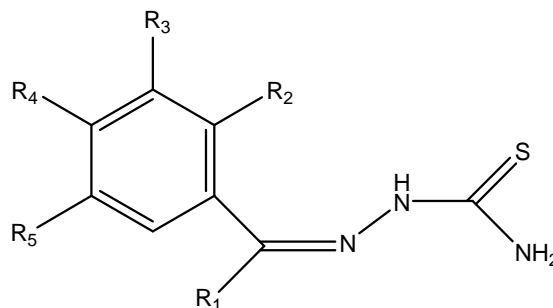


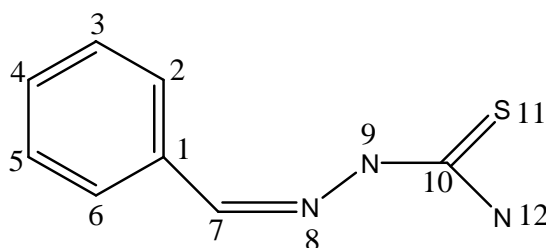
Figure 1: Structure of thiosemicarbazones

Table 1. Selected molecules and their trypanocidal activities

Mol.	R ₁	R ₂	R ₃	R ₄	R ₅	log(IC ₅₀) (μM)
1	Me	H	H	H	H	2.33
2	Me	H	H	OMe	H	1.96
3	Me	Cl	H	H	H	2.30
4	Me	H	H	Cl	H	1.04
5	Me	H	H	H	Br	1.85
6	Me	H	H	Br	H	1.43
7	Me	H	*	*	H	0.98
8	H	H	H	H	H	2.65
9	H	Cl	H	H	H	2.34
10	H	H	Cl	H	H	2.21
11	H	H	H	Cl	H	1.92
12	H	H	H	OMe	H	2.41
13	CH ₂ Me	H	H	OMe	H	2.12
14	H	H	H	Me	H	2.09
15	H	Me	H	H	H	2.35
16	H	OH	H	H	H	2.23
17	H	H	OMe	OH	H	2.47
18	H	OH	H	H	Cl	1.66
19	H	H	Br	H	H	2.13
20	Phe	H	H	H	H	1.83

Calculations

The electronic structure of the molecules was obtained within the Density Functional Theory (DFT) at B3LYP/6-31G(d,p) level with full geometry optimization. The Gaussian suite of programs was employed[45]. The local atomic reactivity indices were calculated from the single point log file with the D-Cent-QSAR software with correction of the anomalous electron populations that sometimes are produced by the Mulliken population analysis[46, 47]. All electron populations smaller than or equal to 0.01e were considered as zero. Orientational parameters of the substituents were calculated as accustomed[31, 32]. We employed the common skeleton (CS) hypothesis stating that there is a particular set of atoms, common to all molecules, which accounts for nearly all the biological activity. The variation of the values of a set of local atomic reactivity indices of a group of atoms belonging to this CS should give an account of the variation of the trypanocidal activity throughout the series analyzed. We made use of Linear Multiple Regression Analysis (LMRA) techniques to determine which atoms and reactivity indices are directly involved in the variation of the biological activity. We built a matrix containing the dependent variable (log (IC₅₀)), and the local atomic reactivity indices of all atoms of the common skeleton as independent variables. The Statistica software was used for LMRA[48]. The common skeleton numbering is shown in Fig. 2.

**Figure 2: Common skeleton numbering**

RESULTS

The LMRA with all molecules gives the following statistically significant equation:

$$\begin{aligned} \log(\text{IC}_{50}) = & -8.89 - 2.52F_2(\text{HOMO})^* + 0.41\mu_4 - 10.25s_5 - 1.93\omega_4 - 0.59\eta_9 \\ & - 0.43F_{10}(\text{LUMO}+1)^* - 0.66F_1(\text{HOMO}-1)^* \end{aligned} \quad (2)$$

with $n=20$, $R=0.98$, $R^2=0.96$, $\text{adj-}R^2=0.93$, $F(7,12)=39.20$ ($p<0.00000$) and a standard error of estimate of 0.12. No outliers were detected and no residuals fall outside the $\pm 2\sigma$ limits. Here $F_2(\text{HOMO})^*$ is the electron population

(Fukui index) of the highest occupied MO localized on atom 2, μ_4 is the local atomic electronic chemical potential of atom 4, s_5 is the local atomic softness of atom 5, ω_4 is the local atomic electrophilicity of atom 4, η_9 is the local atomic hardness of atom 9, $F_{10}(\text{LUMO}+1)^*$ is the Fukui index of the second lowest vacant MO localized on atom 10 and $F_1(\text{HOMO}-1)^*$ is the Fukui index of the second highest occupied MO localized on atom 1.

Table 2 shows the beta coefficients and the *t*-test results for the significance of coefficients of equation 2. Concerning independent variables, Table 3 shows that the highest internal correlation is $r^2(\eta_9, F_2(\text{HOMO})^*)=0.39$. In π conjugated systems it is normal to find a certain degree of correlation between some “independent” variables. Fig. 3 shows the plot of observed values vs. calculated values of $\log(\text{IC}_{50})$. The associated statistical parameters of Eq.2 shows that this equation is statistically significant, explaining about 93% of the variation of the biological activity.

Table 2: Beta coefficients and t-test for significance of coefficients in equation 2

Variable	Beta coefficients	t(12)	p-Value
$F_2(\text{HOMO})^*$	-0.45	-4.89	0.000373
μ_4	0.37	4.69	0.000525
s_5	-0.68	-7.91	0.000004
ω_4	-0.75	-7.36	0.000009
η_9	-0.81	-6.17	0.000048
$F_{10}(\text{LUMO}+1)^*$	-0.35	-4.11	0.001452
$F_1(\text{HOMO}-1)^*$	-0.27	-3.86	0.002249

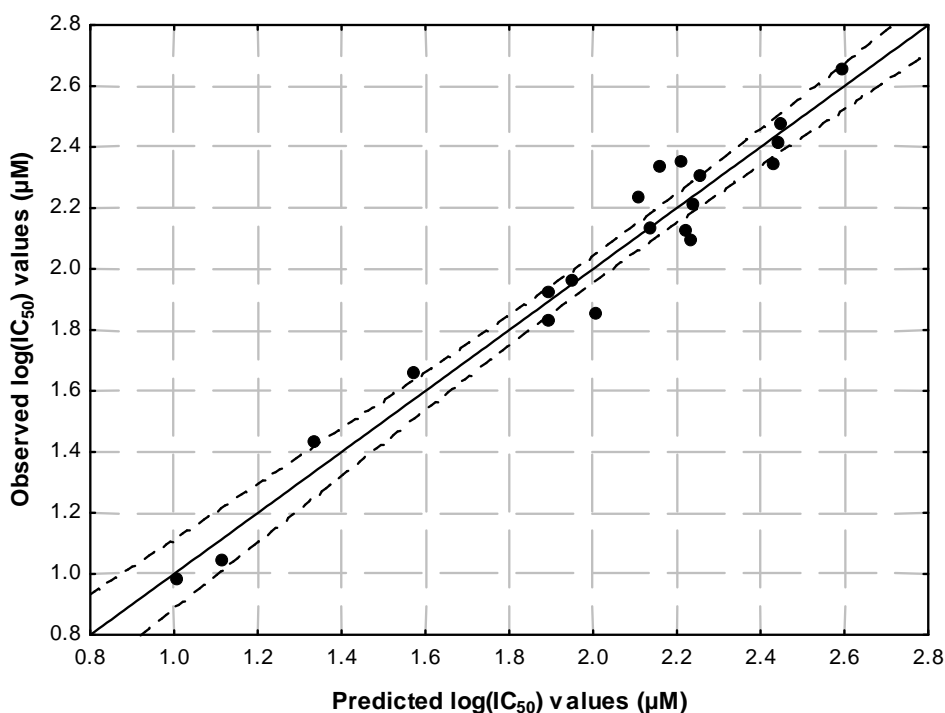


Figure 3: Plot of predicted vs. observed $\log(\text{IC}_{50})$ values. Dashed lines denote the 95% confidence interval

Table 3: Squared correlation coefficients for the variables appearing in equation 2

	$F_2(\text{HOMO})^*$	μ_4	s_5	ω_4	η_9	$F_{10}(\text{LUMO}+1)^*$
μ_4	0.04	1.00				
s_5	0.08	0.006	1.00			
ω_4	0.10	0.30	0.17	1.00		
η_9	0.39	0.32	0.001	0.30	1.00	
$F_{10}(\text{LUMO}+1)^*$	0.18	0.05	0.08	0.003	0.34	1.00
$F_1(\text{HOMO}-1)^*$	0.002	0.0004	0.05	0.01	0.00001	0.06

Table 4 shows the local molecular orbital structure of some atoms appearing in Eq. 2.

Table 4: Local Molecular orbitals of atom 1, 2 and 10

Molecule	Atom 1 (C)	Atom 2 (C)	Atom 10 (C)
1 (51)	47π48π49π-52π53π54π	46π48π49π-52π53π54π	49π50σ51σ-52σ54π55π
2 (59)	56π57π59π-61π62π63π	56π57π59π-60π61π62π	57π58σ59σ-60π61π62π
3 (59)	54π55π56π-60π61π63π	55π56π57π-60π61π62π	57π58σ59σ-60σ61π62π
4 (59)	54π55π56π-60π61π62π	54π56π57π-60π61π62π	57π58σ59σ-60σ62π63π
5 (68)	64π65π66π-69π70π71π	65π66π67π-69π70π71π	66π67σ68σ-69σ71π72π
6 (68)	64π65π66π-69π70π71π	63π65π66π-69π70π71π	66π67σ68σ-69σ71π72π
7 (64)	58π59π60π-65π66π67π	58π59π60π-65π66π67π	62π63σ64σ-65σ66π67π
8 (47)	42π43π45π-48π49π51π	44π45π46π-48π49π51π	45π46σ47σ-48σ49π50π
9 (55)	51π52π53π-56π57π58π	52π53π54π-56π57π58π	53π54σ55σ-56σ58π59π
10 (55)	50π52π53π-56π57π59π	52π53π54π-56π57π58π	53π54σ55σ-56σ58π59σ
11 (55)	51π52π53π-56π57π59π	52π53π54π-56π57π58π	53π54σ55σ-56σ58π60σ
12 (55)	53π54π55π-57π58π59π	53π54π55π-56π57π58π	53π54σ55σ-56π58π59π
13 (63)	59π60π61π-65π67π68π	60π61π62π-64π65π66π	61π62σ63σ-64σ66π67σ
14 (51)	47π48π49π-52π53π54π	47π49π50π-52π53π54π	49π50σ51σ-52π54π55π
15 (51)	47π48π49π-52π53π54π	48π49π50π-52π53π54π	49π50σ51σ-52π54π55π
16 (51)	46π47π49π-52π53π54π	49π50π51π-52π53π54π	48π50σ51σ-52π54π55π
17 (59)	56π57π58π-60π61π62π	57π58π59π-60π61π62π	57π58σ59σ-60π62π63π
18 (59)	55π56π57π-60π61π62π	57π58π59π-60π61π62π	56π58σ59σ-60π62π63π
19 (64)	59π61π62π-65π66π67π	61π62π63π-65π66π67π	62π63σ64σ-65σ67π68π
20 (67)	63π64π65π-69π70π71π	63π64π65π-68π69π70π	65π66σ67σ-68σ72π73σ

DISCUSSION

Our results indicate that for these molecules the variation of the trypanocidal activity on *trypanosomabrucei brucei* is related to the variation of the numerical values of a set of seven local atomic reactivity indices belonging to the common skeleton. This result is very good considering the approximations made to build the model. The Beta values (Table 2) show that the importance of the variables is $\eta_9 > \omega_4 > s_5 > F_2(\text{HOMO})^* > \mu_4 \sim F_{10}(\text{LUMO}+1)^* > F_1(\text{HOMO}-1)^*$ (Table 2). These results are in agreement with the results of the *t*-test (Table 2). The process is orbital-controlled as expected in very specific ligand-site(s) interaction(s). A variable-by-variable analysis indicates that a good trypanocidal activity is associated with high numerical values for $F_2(\text{HOMO})^*$, s_5 , ω_4 , η_9 , $F_{10}(\text{LUMO}+1)^*$ and $F_1(\text{HOMO}-1)^*$. This is so because all these variables have positive numerical values and are accompanied by a minus sign in Eq.2. μ_4 has negative values but it has a plus sign accompanying it. Therefore a good trypanocidal activity is associated with a very negative value for this index. First, we shall analyze the MO-independent local atomic reactivity indices. Atom 9 is a nitrogen one (Fig. 2). A high value for η_9 indicates that the HOMO*-LUMO* energy distance is large. Therefore atom 9 seems to resist exchanging electrons with the surroundings. This, in turn, allows suggesting that atom 9 is possibly situated close to a hydrophobic moiety (an alkyl chain for example). Atom 4 is a carbon atom of the phenyl moiety (Fig. 2). ω_4 is the local atomic electrophilicity of atom 4. The condition of a high value for ω_4 indicates that this atom is interacting with an electron-rich center. This is in perfect agreement for the requirement of a highly negative value for μ_4 because if the associated HOMO₄* eigenvalue is shifted downwards in the energy axis, then this atom is more prone to receive electrons. Atom 5 is carbon atom of the phenyl moiety (Fig. 2). s_5 is defined as the inverse of the (HOMO)₅*-(LUMO)₅* energy gap. Therefore, a high value for s_5 suggests that atom 5 is interacting with an electron-deficient center. This interaction can be of the π -cation or π - π kinds. Now, we shall analyze the MO-dependent atomic reactivity indices. Atom 1 is a carbon of the phenyl moiety (Fig. 2). (HOMO-1)₁* and (HOMO)₁* are MOs of π nature (Table 4). Fig. 4 shows the case of molecule 1. The fact that (HOMO-1)₁* appears in the equation indicates that (HOMO)₁* is also participating. Therefore a high value for $F_1(\text{HOMO}-1)^*$ suggests that the two highest occupied local MOs are interacting with an electron-deficient center, such as a cation or an aromatic moiety (a π - π interaction). Atom 2 is a carbon atom of the phenyl moiety (Fig. 2). (HOMO)₂* is a π MO (Table 4), the example for molecule 2 is showed in figure 5. A high value for $F_2(\text{HOMO})^*$ indicates that atom 2 is interacting with an electron-deficient center such as part of an aromatic moiety or a cation. Atom 10 is a carbon atom (Fig. 2). (LUMO)₁₀* is a σ MO in almost all molecules and (LUMO+1)₁₀* is a π MO in all them (Table 4). Fig. 6 shows the case of molecule 3. A high value for $F_{10}(\text{LUMO}+1)^*$ suggests that

(LUMO+1)₁₀* is interacting with a site rich in electrons. Considering that (LUMO)₁₀* also participates in the process, it could be interacting with another site containing occupied sigma MOs such as methylene groups.

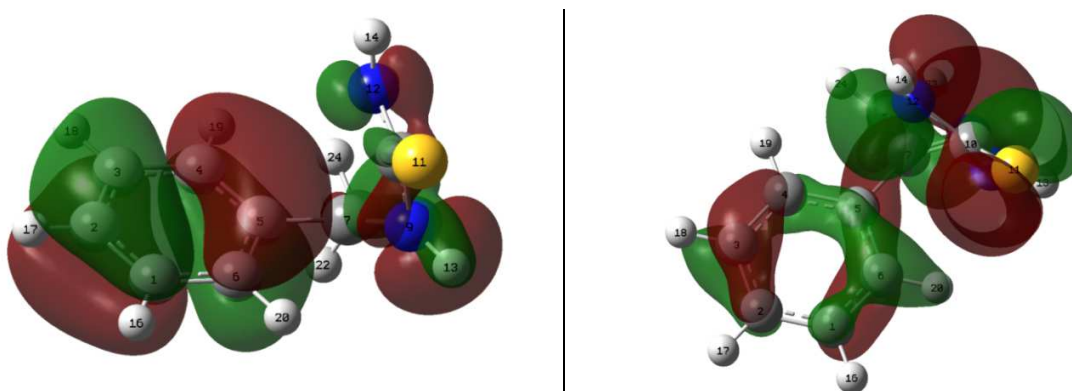


Figure 4: Left: Local (HOMO-1)* of atom 1 in molecule 1 (corresponding to the molecule's (HOMO-3)). Right: Local (HOMO)* of atom 1 in molecule 1 (corresponding to the molecule's (HOMO-2))

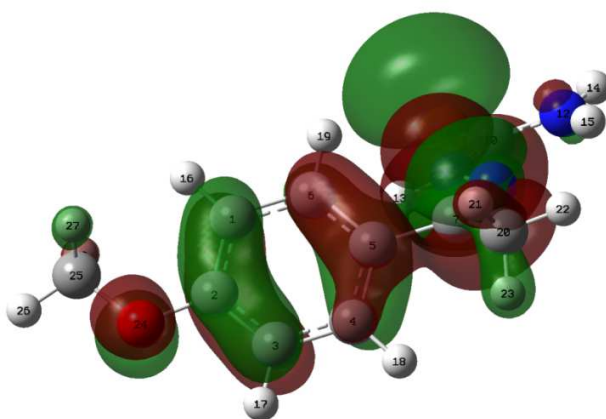


Figure 5: Local (HOMO)* of atom 2 in molecule 2 corresponding to the molecule's HOMO

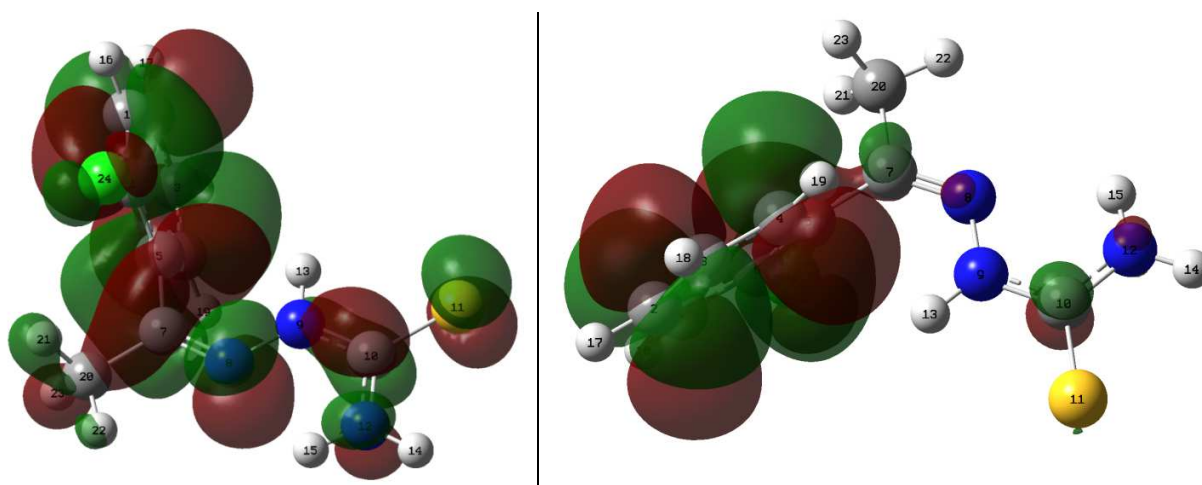


Figure 6: Left: Local (LUMO)* of atom 10 in molecule 3 (corresponding molecule's (LUMO)). Right: Local (LUMO+1)* of atom 10 in molecule 3 (corresponding molecule's (LUMO+1))

This analysis allows us to propose the following 2D pharmacophore for the trypanocidal activity of thiosemicarbazone derivatives on *Trypanosome brucei-brucei*.

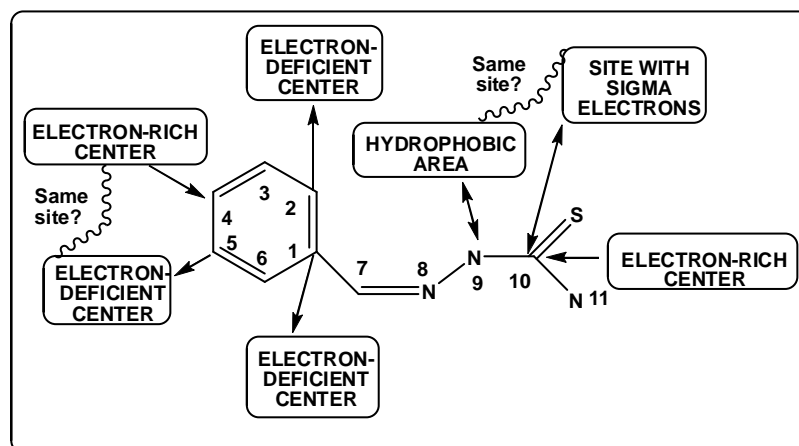


Figure 7: Proposed 2D pharmacophore for the trypanocidal activity of thiosemicarbazone derivatives on *trypanosome brucei-brucei*

CONCLUSION

We have obtained statistically significant results relating the variation of a definite set of local atomic reactivity indices to the variation of trypanocide activity on *Trypanosoma brucei brucei* for a series of thiosemicarbazone derivatives. The whole process seems to be orbital-controlled[49]. The results should be useful to propose new molecules which higher trypanocide activity.

REFERENCES

- [1] R. Vicik, V. Hoerr, M. Glaser, M. Schultheis, E. Hansell, J. H. McKerrow, U. Holzgrabe, C. R. Caffrey, A. Ponte-Sucre, H. Moll, A. Stich, T. Schirmeister, *Bioorg. Med. Chem. Lett.*, **2006**, 16, 2753-2757.
- [2] S. Ellis, D. W. Sexton, D. Steverding, *Exp. Parasitol.*, **2015**, 150, 7-12.
- [3] H. R. Fatondji, S. Kpoviessi, F. Gbaguidi, J. Bero, V. Hannaert, J. Quetin-Leclercq, J. Poupaert, M. Moudachirou, G. C. Accrombessi, *Med. Chem. Res.*, **2013**, 22, 2151-2162.
- [4] WHO, "Trypanosomiasis, human African (sleeping sickness)," February 2016, <http://www.who.int/mediacentre/factsheets/fs259/en/>.
- [5] S. R. Wilkinson, J. M. Kelly, *Exp. Rev. Mol. Med.*, **2009**, 11.
- [6] D. Steverding, *Paras. Vect.*, **2010**, 3, 15.
- [7] D. K. Sau, R. J. Butcher, S. Chaudhuri, N. Saha, *Mol. Cell. Biochem.*, **2003**, 253, 21-29.
- [8] A. P. Rebolledo, G. M. de Lima, L. N. Gambi, N. L. Speziali, D. F. Maia, C. B. Pinheiro, J. D. Ardisson, M. E. Cortés, H. Beraldo, *App. Organomet. Chem.*, **2003**, 17, 945-951.
- [9] N. C. Kasuga, K. Sekino, M. Ishikawa, A. Honda, M. Yokoyama, S. Nakano, N. Shimada, C. Koumo, K. Nomiya, *J. Inorg. Biochem.*, **2003**, 96, 298-310.
- [10] C. C. García, B. N. Brousse, M. J. Carlucci, A. G. Moglioni, M. M. Alho, G. Y. Moltrasio, N. B. D'Accorso, E. B. Damonte, *Antivir. Chem. Chemother.*, **2003**, 14, 99-105.
- [11] D. Kovala-Demertzi, M. A. Demertzi, J. R. Miller, C. S. Frampton, J. P. Jasinski, D. X. West, *J. Inorg. Biochem.*, **2002**, 92, 137-140.
- [12] Z. Afrasiabi, E. Sinn, J. Chen, Y. Ma, A. L. Rheingold, L. N. Zakharov, N. Rath, S. Padhye, *Inorg. Chim. Acta*, **2004**, 357, 271-278.
- [13] Z. Afrasiabi, E. Sinn, S. Padhye, S. Dutta, S. Padhye, C. Newton, C. E. Anson, A. K. Powell, *J. Inorg. Biochem.*, **2003**, 95, 306-314.
- [14] M. IC, M. JP, Speziali NL, M. AS, T. JA, B. H., *J. Braz. Chem. Soc.*, **2006**, 17, 1571-1577.
- [15] D. C. Greenbaum, Z. Mackey, E. Hansell, P. Doyle, J. Gut, C. R. Caffrey, J. Lehrman, P. J. Rosenthal, J. H. McKerrow, K. Chibale, *J. Med. Chem.*, **2004**, 47, 3212-3219.

- [16] X. Du, C. Guo, E. Hansell, P. S. Doyle, C. R. Caffrey, T. P. Holler, J. H. McKerrow, F. E. Cohen, *J. Med. Chem.*, **2002**, 45, 2695-2707.
- [17] N. Fujii, J. P. Mallari, E. J. Hansell, Z. Mackey, P. Doyle, Y. M. Zhou, J. Gut, P. J. Rosenthal, J. H. McKerrow, R. K. Guy, *Bioorg. Med. Chem. Lett.*, **2005**, 15, 121-123.
- [18] I. Chiyanzu, E. Hansell, J. Gut, P. J. Rosenthal, J. H. McKerrow, K. Chibale, *Bioorg. Med. Chem. Lett.*, **2003**, 13, 3527-3530.
- [19] C. R. Caffrey, S. Scory, D. Steverding, *Current Drug Targets*, **2000**, 1, 155-162.
- [20] J. P. Mallari, A. Shelat, A. Kosinski, C. R. Caffrey, M. Connelly, F. Zhu, J. H. McKerrow, R. K. Guy, *Bioorg. Med. Chem. Lett.*, **2008**, 18, 2883-2885.
- [21] J. S. Gómez-Jeria, *Boll. Chim. Farmac.*, **1982**, 121, 619-625.
- [22] J. S. Gómez-Jeria, *Int. J. Quant. Chem.*, **1983**, 23, 1969-1972.
- [23] J. S. Gómez-Jeria, "Modeling the Drug-Receptor Interaction in Quantum Pharmacology," in *Molecules in Physics, Chemistry, and Biology*, J. Maruani Ed., vol. 4, pp. 215-231, Springer Netherlands, **1989**.
- [24] C. Barahona-Urbina, S. Nuñez-Gonzalez, J. S. Gómez-Jeria, *J. Chil. Chem. Soc.*, **2012**, 57, 1497-1503.
- [25] T. Bruna-Larenas, J. S. Gómez-Jeria, *Int. J. Med. Chem.*, **2012**, 2012 Article ID 682495, 1-16.
- [26] J. S. Gómez-Jeria, *Elements of Molecular Electronic Pharmacology (in Spanish)*, Ediciones Sokar, Santiago de Chile, 2013.
- [27] J. S. Gómez-Jeria, *Canad. Chem. Trans.*, **2013**, 1, 25-55.
- [28] J. S. Gómez-Jeria, M. Flores-Catalán, *Canad. Chem. Trans.*, **2013**, 1, 215-237.
- [29] K. Fukui, H. Fujimoto, *Frontier orbitals and reaction paths: selected papers of Kenichi Fukui*, World Scientific, Singapore; River Edge, N.J., **1997**.
- [30] J. S. Gómez-Jeria, M. Ojeda-Vergara, *J. Chil. Chem. Soc.*, **2003**, 48, 119-124.
- [31] J. S. Gómez-Jeria, *Res. J. Pharmac. Biol. Chem. Sci.*, **2016**, 7, 288-294.
- [32] J. S. Gómez-Jeria, *Res. J. Pharmac. Biol. Chem. Sci.*, **2016**, 7, 2258-2260.
- [33] M. S. Leal, A. Robles-Navarro, J. S. Gómez-Jeria, *Der Pharm. Lett.*, **2015**, 7, 54-66.
- [34] J. Valdebenito-Gamboa, J. S. Gómez-Jeria, *Der Pharma Chem.*, **2015**, 7, 543-555.
- [35] H. R. Bravo, B. E. Weiss-López, J. Valdebenito-Gamboa, J. S. Gómez-Jeria, *Res. J. Pharmac. Biol. Chem. Sci.*, **2016**, 7, 792-798.
- [36] J. S. Gómez-Jeria, S. Abarca-Martínez, *Der Pharma Chem.*, **2016**, 8, 507-526.
- [37] J. S. Gómez-Jeria, H. R. Bravo, *Der Pharma Chem.*, **2016**, 8, 25-34.
- [38] J. S. Gómez-Jeria, R. Cornejo-Martínez, *Der Pharma Chem.*, **2016**, 8, 329-337.
- [39] J. S. Gómez-Jeria, V. Gazzano, *Der Pharma Chem.*, **2016**, 8, 21-27.
- [40] J. S. Gómez-Jeria, M. Matus-Perez, *Der Pharma Chem.*, **2016**, 8, 1-11.
- [41] J. S. Gómez-Jeria, C. Moreno-Rojas, *Der Pharma Chem.*, **2016**, 8, 475-482.
- [42] J. S. Gómez-Jeria, Í. Orellana, *Der Pharma Chem.*, **2016**, 8, 476-487.
- [43] G. A. Kpotin, G. S. Atohoun, U. A. Kuevi, A. Houngue-Kpotia, J.-B. Mensah, J. S. Gómez-Jeria, *J. Chem. Pharmaceut. Res.*, **2016**, 8, 1019-1026.
- [44] A. Robles-Navarro, J. S. Gómez-Jeria, *Der Pharma Chem.*, **2016**, 8, 417-440.
- [45] M. J. Frisch, G. W. Trucks, H. B. Schlegel, G. E. Scuseria, M. A. Robb, J. R. Cheeseman, J. Montgomery, J.A., T. Vreven, K. N. Kudin, J. C. Burant, J. M. Millam, S. S. Iyengar, J. Tomasi, V. Barone, B. Mennucci, M. Cossi, G. Scalmani, N. Rega, "G03 Rev. E.01," Gaussian, Pittsburgh, PA, USA, **2007**.
- [46] J. S. Gómez-Jeria, *J. Chil. Chem. Soc.*, **2009**, 54, 482-485.
- [47] J. S. Gómez-Jeria, "D-Cent-QSAR: A program to generate Local Atomic Reactivity Indices from Gaussian 03 log files. v. 1.0," Santiago, Chile, **2014**.
- [48] Statsoft, "Statistica v. 8.0," 2300 East 14 th St. Tulsa, OK 74104, USA, **1984-2007**.
- [49] G. Klopman, *J. Am. Chem. Soc.*, **1968**, 90, 223-234.